Indoor-to-Outdoor Empirical Path-loss Modelling for Femtocell Networks at 0.9, 2, 2.5 and 3.5 GHz using Singular Value Decomposition

Ben Allen, Shyam Mahato, Y Gao, S Salous

E-mail: Ben.Allen@eng.ox.ac.uk

Abstract

Two empirical indoor-to-outdoor path-loss models to facilitate femtocell network deployment are derived from Continuous Wave (CW) power measurements. A large set of indoor/outdoor transmitter locations in two residential streets in an urban setting and operating at 900 MHz, 2 GHz, 2.5 GHz and 3.5 GHz have been used to derive the model parameters by using Singular Value Decomposition (SVD). The two models provide a trade-off between available degrees-of-freedom, complexity and accuracy; where a model may be selected according to the given operating scenario and frequency. The path-loss models have been compared and validated against existing models as well as independent measurement data, and considered in terms of residual error and key parameters such as path-loss exponent, and good comparison is shown. The Root Mean Square Error (RMSE) of the residual path loss data obtained from the measurement data, which directly relates to the channel shadowing characteristics, is compared and validated with known results in terms of standard deviation and probability density function, and has led to new model parameters being proposed. The expressions derived from the modelling can be used in system-level simulators, as well as for interference analysis of two-tier heterogeneous networks operating in indoor-outdoor scenarios at or close to the operating frequencies considered in this paper. The models in this paper extend the operating frequency range compared to related models and introduces SVD as a convenient means of deriving parameters from measured path-loss data.

B Allen is with the Department of Engineering Science, University of Oxford, OX1 3PJ, UK.

S. Mahato was with the Institute for Research in Applicable Computing, University of Bedfordshire, LU1 3JU, Luton, UK.

Y Gao is with the School of Electronics and Information, Northwestern Polytechnical University, Xi'an, China

S Salous is with the School of Engineering and Computing Sciences, Durham University, Durham, UK

Indoor-to-Outdoor Empirical Path-loss Modelling for Femtocell Networks at 0.9, 2, 2.5 and 3.5 GHz using Singular Value Decomposition

I. Introduction

As the demand for spectrum within the context of mobile wireless networks continues to grow, low-power base stations, also known as Femtocell Access Points (FAP), have become an important means of increasing spectrum efficiency. They have been shown to improve indoor coverage and capacity such as inside a residential house, in a shopping mall, in an airport and in a train station [1]. The deployment of co-channel femtocells over a macrocell network imposes interference to the macrocell users. In order to estimate this interference and to consequently ensure optimum network design and operation, a suitable propagation model is needed. Such a model would need to provide a reliable estimate of received power at a given distance from the transmitter, with sufficient accuracy to enable robust design and deployment of network equipment. The model should reflect typical operational scenario, i.e., indoor, indoor-to-outdoor, operating frequency, physical environment etc. It is also preferable that the model is computational succinct whilst providing the required accuracy.

In this paper, the indoor-to-outdoor radio propagation in terms of path-loss for a femtocell network has been studied for two residential areas in an urban environment whilst operating at four different carrier frequencies pertinent to the deployment of femtocells. The measured received signal power was used to form two empirical path-loss models for each frequency. Model A includes losses due to walls, whereas Model B additionally distinguishes between the indoor and outdoor regions. The modelling process uses Least Squares Fit by means of Singular Value Decomposition (SVD) [2] [3] to determine the model parameters. This technique has been used extensively in wireless communications to determine MIMO channel parameters, channel capacity and antenna beamforming weights [4]. In this paper, however, the same mathematical technique has been adopted for path-loss model parameter estimation. Furthermore, the residual path-loss obtained from the measurement data was analysed in terms of Root Mean Square Error (RMSE) to enable the channel shadowing to be characterised. The resulting path-loss and shadowing models may subsequently be used as analytic expressions to estimate the level of interference between users, which may be part of a network level simulation or on an individual link basis.

Several empirical path-loss models for indoor-to-outdoor channels can be found in the literature, such as in references [5]–

[13]. However, none of the models have adopted SVD as a means of determining path-loss and shadowing model parameters from data, nor encompassed models derived from a single measurement campaign covering four operating frequencies and explicitly include indoor signal attenuation as a factor. Reference [5] provides a review of many of these models and related modelling methodologies. Each model has its own restriction in terms of frequency range, environment or modelling approach. For example, the path-loss model developed in [6] is suitable for the frequency ranges 5-6 GHz. It has been derived by parameter fitting using Minimum Mean Squared Error (MMSE) and Least Squares Error (LSE), where the problem has been formulated and manipulated using matrices. Hence, this approach is akin to (but does not use) the SVD methodology adopted in this paper. In comparison, we use SVD to provide a direct solution to LMS parameter estimation. Rose, *et al.* in [7], carried out extensive measurements to study the indoor-to-outdoor propagation of Long-Term Evolution (LTE) femtocells at 800 MHz and 2600 MHz frequencies, but the paper has not presented an analytical model. Instead, the extensive measurement set is used to directly indicate path-loss over the scenarios of interest. In [8], the WINNER II project studied the propagation behaviour under various scenarios in a university setting. The measurements were conducted in the frequency range of 2-6 GHz and does not extend down to 900 MHz. The antennas were 2 m and 2.5 m above the ground and residential settings were not considered. Linares, in [9], developed an empirical path-loss model for Femto-to-UE links for evaluation of Femto-to-Macro interference scenarios at 2.4 GHz, where only a single frequency of 2.4 GHz was considered in the reference. In [10], an analytical expression for the additional losses from the indoor/outdoor interface was developed based on the statistics extracted from ray-tracing simulations, and it had not been validated against measurements. Further, the model does not use the SVD methodology that is used in this paper. Another model that is described in [14] uses a combination of ray tracing and Finite Difference Time Domain techniques to compute the indoor-outdoor path-loss. Whilst this work focusses on 3.5 GHz, it could in principal be utilised at a range of other frequencies and operating environments provided the necessary data is available, which is also the case for the model described in [10], . These two techniques carry a high computational requirement compared to the model described in this paper. The International Telecommunication Union - Radiocommunications (ITU-R), in recommendation [11], provides guidance on indoor propagation over the frequency range from 900 MHz to 100 GHz. This recommendation considers only the indoor propagation channel and not the indoor-to-outdoor channel, although an extensive frequency range has been incorporated in the recommendation. It is recommended that indoor-to-outdoor propagation analysis should make use of this recommendation as well as a related recommendation that covers the outdoor segment. Despite this, explicit guidance and model for the complete channel is not given. Another ITU Recommendation [15], provides definitions of building entry loss and measurement methods. However, neither actual values of loss or models are provided. Corre and Stephan, in [12], proposed two different indoor-to-outdoor path-loss models at 2.1 GHz. The approach uses ray-tracing together

with an analytic parametric model. Only a single frequency band has been considered and not all of the work has been validated by measurements.

From the literature review, it is noted that many papers have studied the propagation behaviour of the indoor-to-outdoor channel for the higher frequencies and has not considered the lower frequencies such as 900 MHz, which is under trial for LTE-Advanced in some countries. For example, Telstra and Ericsson in Australia made the world's first commercial LTE-Advanced call in the 900 MHz spectrum band on 31st July 2013 [16]. We note, however, that there are practical difficulties in using such frequencies for these deployments. For example, the antenna form-factor becomes larger and favorable propagation conditions results in cross-layer interference being higher than when operating at higher frequencies. Valcarce, in [13], has developed an empirical indoor-to-outdoor path-loss model for certain frequencies in the range of 900 MHz to 3.5 GHz. The model is a general expression in terms of frequency and the number of walls, which has been generated using the *trust region* optimisation curve fitting technique. This model does not explicitly incorporate propagation attenuation inside the building. The work presented in this paper, however, uses the same data-set as the empirical models proposed in [13], but we extend the work by adopting the SVD-based methodology. We derive a model that incorporates indoor signal attenuation as a key parameter, and also investigate the investigate channel shadowing parameters, where results are conveniently obtained as a consequence of using the SVD method. We validate our proposed empirical models against those in [13] and against independently measured path-loss data using the University of Durham's channel sounder described in [17].

In this paper, we consider the major contributions to be:

- applying SVD for deriving model parameters from the measurement data, which, although it is very well understood for extracting MIMO sub-channels, it has not, to the best of our knowledge, been considered in the existing path-loss modelling literature to date;
- defining and validating two path-loss models (equations 7, 9 with parameters given in tables II, and III respectively) at four different carrier frequencies, which consider losses due to walls and the propagation inside the building. The second and most refined model explicitly considers the individual contributions of the outdoor propagation loss, loss due to walls and the indoor propagation loss;
- deriving a shadowing model and characteristics in terms of the frequency dependent behaviour, i.e., shadowing is modelled and characterised for carrier frequencies of 0.9, 2, 2.5 and 3.5 GHz, and conveniently derived as a consequence of using the proposed SVD method.This is a new addition and not considered in [13]

The paper is structured as follows. Section II describes the procedure followed in the measurement campaign. The modelling of the data to produce the parameters for the empirical path-loss models is presented in Section III, followed by the results

and validation of the modelled parameters in Section IV. Finally, Section V concludes the paper.

II. Measurement Campaign

Received CW power measurements were conducted and presented in [13] and [18] that study several wireless operating scenarios and at carrier frequencies of 900 MHz, 2 GHz, 2.5 GHz and 3.5 GHz. These measurements have formed the basis of the empirical path-loss modelling activity detailed in this paper. Unlike the path-loss model described in [13], these new models use the SVD technique to extract the channel parameters. The resulting models encompass operating frequencies in the range of 900 MHz to 3.5 GHz and explicitly account for parameters such as wall losses and indoor propagation loss.

A. Measurement Equipment

The equipment,configuration and operation is described as follows, where the system configuration is detailed in Table I.

1) Antennas: The antennas used at the transmitter and the receiver were slim flexible dipoles from *Cobham* [19]. The single-band antennas for each of the centre frequencies have similar omni-directional radiation patterns with a vertical beamwidth of 80° and a maximum gain of 2 dBi. Both transmit and receive antennas were orientated vertically for all of the measurements.

2) Vector Signal Generator: A Vector Signal Generator from Anritsu (model MG3700A) was used to generate CW signals at the frequencies of interest.

3) Spectrum Analyser: A Spectrum Analyser from Anritsu (type MS2721B) was used as a receiver to measure the received power. This is a portable device with an integrated Global Positioning System (GPS) module which was used to record the location of each measurement.

B. Measurement Environment and Scenarios

The measurements were conducted in Luton, United Kingdom. Two residential streets were chosen for the measurement: Russell Rise (RR) and Stockwood Crescent (SC), where the houses along the street have 2-3 floors with an average roof height of 6 m. The outer walls are typically made of brick, whereas the inner walls are made of wood, chipboard and plaster [13]. The signal will also find paths through doors (typically made of wood) and windows (single or double glazed).

Three different scenarios of transmitter locations for the two houses of interest (one along RR and the other along SC) are described below. The receiver was portable along the test routes described later in this section. The transmit and receive antennas were 1 m and 1.2 m above the street respectively, which is considered to be representative of a femtocell and mobile user deployment.

- Scenario 1: The transmitter was placed outside and in front of the outer facade of a terraced house near the edge of the road. This scenario allows for the impact of the walls to be explicitly included in the models.

- Scenario 2: The transmitter was placed on the ground floor inside the building in the first room from the road, where the direct radio path between the transmitter and the road includes one wall (referred to as *BR* or Bedroom in Fig. 1).
- Scenario 3: The transmitter was placed on the ground floor inside the building in the second room from the road, where the shortest radio path between the transmitter and the road includes two walls (referred to as *LR* or Livingroom in Fig. 1).

An aerial view of the measurement streets using the Google Earth tool is shown in Fig. 1 which shows the test houses and three scenarios of the transmitter locations in each street. The white line along the pedestrian path represents the measurement route that the portable receiver followed.

(a) Street 1: Russel Rise (RR) (b) Street 2: Stockwood Crescent (SC)

Fig. 1. Transmitter locations and route of the portable receiver (©Bluesky International Ltd, 2013)

TABLE I

PARAMETERS FOR MEASUREMENT SETTINGS

Measurement Parameters	Value
Carrier frequencies	0.9, 2.0, 2.5, 3.5 GHz
Transmitter output power	19 dBm
Transmitter/Receiver antenna's gain	2 dBi
Transmitter antenna height	1 m above the floor level
Receiver antenna height	$\approx$ 1.2 m above the street
Resolution bandwidth	9 Hz
Sweep rate	1 kHz

C. Measurement Methodology

The measurement receiver was carried by hand in order to resemble realistic usage of user equipment (UE) and walked along the pedestrian routes shown in Fig 1, with the user located so as to minimise the possibility of additional body loss

influencing the measurements. The measurements have been performed along the street immediately adjacent to the premises in order to determine the leakage power from a femtocell placed inside a nearby house and until the distance at which the received channel power drops below -110 dBm with 10 dB link margin from the noise floor at -120 dBm [13]. Note that a line-of-sight signal path exists for some locations to the front of the house for both scenarios. Occlusions occur due to parked cars and a curve in the road of scenario 2. The measurements were conducted for each location with a frequency sweep of 1 kHz centred at the chosen carrier frequency. This ensures the operating bandwidth is wide enough to encompass frequency instability of the transmitter, as well as Doppler shift and allows for signal averaging to take place. The receiver was configured to record the spectrum at intervals of 9 Hz and the net received power was computed by integrating the recorded points over the spectral band. Since the receiver detector provided an integration process, moving at the pace of the pedestrian operator (approximately 2.5 m/s) provided an averaging function to suppressed the effect of small-scale fading on the measured data. The locations of the measurements were simultaneously logged using a GPS receiver [13]. Around 4000 data values were collected and used to provide input data for the subsequent models to be derived from.

Both the measurement data and GPS data were subject to fading. Thus the data was processed to correct the 'outlier' GPS data points and remove 'outlier' received channel power data i.e., the received signal strength fell below the link threshold of -110 dBm.

III. Empirical Path-loss Modelling

Here, the underlying path-loss model is described, together with the modelling methodology. The aim is to derive an empirical model that describes path-loss as a function of distance between the transmitter and receiver. The approach taken here uses the SVD methodology to succinctly compute model parameters from the measured data by means of LMS parameter estimation. Two models are described, where each have parameters (and hence degrees-of-freedom) to account for specific aspects of the scenario, such as average wall loss and internal propagation loss.

SVD [2] is a mathematical method that can be used to decompose a matrix into simpler forms, which may then be attributed to a physical meaning used to provide insights such as the path-loss exponent, average wall loss etc. It provides a means of Least Mean Squares fitting of data and parameter estimation [3], which is why it has been used here. It operates by minimising the sum of the squares of the residuals, where a residual is the difference between a measured and fitted value. SVD is well known in the area of wireless communications as it has been used extensively as a means of extracting insights into the behaviour of MIMO spatial channels and configuring MIMO arrays [4]. However, it is used here to compute model parameters from radio channel path-loss data.

After processing the measured received signal power data as described in the previous section, the data was used to develop

the empirical path-loss models. From the measurement of the received power data, the path-loss, L_p, can be calculated as

$$L_p = P_{tx} + G_{tx} + G_{rx} - P_{rx} \quad \text{[dB]}, \tag{1}$$

where $P_{tx} = 19$ dBm is the transmitter power, $G_{tx} = 2$ dBi is the gain of the transmitter antenna, $G_{rx} = 2$ dBi is the gain of the receiver antenna and P_{rx} is the measured received power in dBm. The process of modelling the calculated path-loss data is described as follows.

- Linear Least-Square fit using the SVD algorithm [3] [2] was used to fit the measurement data. The SVD algorithm operates with the following construct,

  $$\boldsymbol{L_p} = \boldsymbol{DC} + \boldsymbol{e}, \tag{2}$$

  where $\boldsymbol{L_p}$ is an $n \times 1$ vector of the calculated path-loss data from the measurement data, n represents the number of measurement points; $\boldsymbol{D}$ is an $n \times m$ design matrix for a model where m represents the number of the modelled parameters, $\boldsymbol{C}$ is an $m \times 1$ vector of unknown coefficients of the model and $\boldsymbol{e}$ is an $n \times 1$ vector of the residual path-loss data obtained from the resultant difference bewteen the measurement data and values provided by the resulting model.
- The solution of the unknown model coefficients is obtained by the SVD algorithm as

  $$\boldsymbol{C} = (\boldsymbol{D}^\top \boldsymbol{D})^{-1} \boldsymbol{D}^\top \boldsymbol{L_p}, \tag{3}$$

  where $(\cdot)^\top$ represents the transpose of the matrix, while $(\cdot)^{-1}$ represents the inverse.
- The residual path-loss data from the measured data and the fitted model can be obtained as

  $$\boldsymbol{e} = (\boldsymbol{I} - \boldsymbol{H})\boldsymbol{L_p}, \tag{4}$$

  $$\boldsymbol{H} = \boldsymbol{D}(\boldsymbol{D}^\top \boldsymbol{D})^{-1} \boldsymbol{D}^\top, \tag{5}$$

  where $\boldsymbol{I}$ represents $n \times n$ identity matrix, $\boldsymbol{e}$ represents $n \times 1$ vector of the residual data obtained from the difference between measurement data and values obtained from the resulting model, and $\boldsymbol{H}$ is an $n \times n$ matrix determined from the design matrix, $\boldsymbol{D}$.
- The residual path-loss data was analysed with the minimum Root Mean Square Error (RMSE) as

  $$r = \sqrt{\frac{\boldsymbol{e}^\top \boldsymbol{e}}{n}}, \tag{6}$$

  where r is the standard deviation of the residual path loss data in dB which is the RMSE value as described later in the paper.

The estimated path loss data was modelled in two different ways: *Model A* (includes the effect of the wall attenuation) and *Model B* (includes the effect of wall attenuation as well as indoor propagation loss), and described as follows.

A. Path-loss Model A

In this model, the losses due to the walls are modelled separately. The measurement data from all three transmitter locations (outdoor, bedroom and living-room) are used. The estimated path-loss data is modelled as

$$L_p = \alpha + 10\beta \log_{10}(d) + \gamma w + \sigma, \tag{7}$$

where γ is the average attenuation coefficient in dB per wall, w is the number of walls between the transmitter and the receiver and σ represents the standard deviation in dB of the log-normal shadow fading. In this model, the modelled parameters are α, β and γ, i.e., 3 degrees-of-freedom. The design matrix and the coefficient vector are expressed as

$$\boldsymbol{D} = \begin{bmatrix} 1 & 10\log_{10}(d_1) & w \\ 1 & 10\log_{10}(d_2) & w \\ \vdots & \vdots & \vdots \\ 1 & 10\log_{10}(d_n) & w \end{bmatrix} \text{ and } \boldsymbol{C} = \begin{bmatrix} \alpha \\ \beta \\ \gamma \end{bmatrix}, \tag{8}$$

where d_n is the distance between the receiver and the transmitter , and w is the number of the walls between the transmitter and the receiver at point n, i.e., 0, 1 or 2.

B. Path-loss Model B

In this model, the losses due to the walls and the propagation inside the building are modelled separately and repeated for each carrier frequency. The estimated path-loss data is modelled as

$$L_p = \alpha + 10\beta \log_{10}(d) + \gamma w + \delta d_{in} + \sigma, \tag{9}$$

where δ is the distance attenuation coefficient in dB/m corresponding to the distance inside the building and d_{in} is the propagation distance inside the building from the transmitter to the wall. In this model, the parameters are α, β, γ and δ, i.e., 4 degrees-of-freedom. The design matrix and the coefficient vector are expressed as

$$\boldsymbol{D} = \begin{bmatrix} 1 & 10\log_{10}(d_1) & w & d_{in} \\ 1 & 10\log_{10}(d_2) & w & d_{in} \\ \vdots & \vdots & \vdots & \vdots \\ 1 & 10\log_{10}(d_n) & w & d_{in} \end{bmatrix} \text{ and } \boldsymbol{C} = \begin{bmatrix} \alpha \\ \beta \\ \gamma \\ \delta \end{bmatrix}. \tag{10}$$

The measurement data from Scenario 2 (Tx in BR) and Scenario 3 (Tx in LR) were modelled in two steps. This enables the indoor and outdoor losses to be considered seperatly, and consequently used separately as required. It also enables an additional degree of freedom to be utilised in the model, thus giving the potential for improving the model accuracy and retaining a

physical meaning of the model's parameters. In the first step, the modelled parameters, α and β, where α is a constant in dB which is the path-loss at a reference distance, β is the path-loss exponent, d is the distance in meters between the transmitter and the receiver were used to determine the path-loss between the front face of the building and the receiver position, i.e., data points relating to indoor locations where excluded. In the second step, the excess path-loss was determined by subtracting the outdoor path-loss (scenario 1) from the measured path-loss of Scenario 2 (1 wall) and Scenario 3 (2 walls) respectively. Then, the excess path-loss data was modelled as a loss due to the walls and the propagation inside the building. That is,

- Path-loss outside:

$$L_{out} = \alpha + 10\beta \log_{10}(d_{ref-rx}), \tag{11}$$

  where L_{out} is the path-loss outside the building, d_{ref-rx} is the distance between the reference point (i.e., the front face of the building) and the receiver location.

- Path loss inside:

$$L_{in} \quad = \quad L_{meas} - L_{out} = \gamma w + \delta d_{in}, \tag{12}$$

  where L_{in} is the excess path-loss obtained by subtracting the path-loss outside the building from the measured path-loss when the transmitter was placed inside the building, L_{meas} is the path-loss measured in the case of the transmitter placed inside the building.

Therefore, the combined path-loss in the case of the transmitter placed inside the building can be written as

$$L_p \quad = \quad L_{out} + L_{in}. \tag{13}$$

The design matrix and the coefficient vector for this model are expressed as

- Path-loss outside:

$$\boldsymbol{D}_{out} = \begin{bmatrix} 1 & 10\log_{10}(d_{ref-rx_1}) \\ 1 & 10\log_{10}(d_{ref-rx_2}) \\ \vdots & \vdots \\ 1 & 10\log_{10}(d_{ref-rx_n}) \end{bmatrix} \text{ and } \boldsymbol{C}_{out} = \begin{bmatrix} \alpha \\ \beta \end{bmatrix}. \tag{14}$$

- Path loss inside:

$$\boldsymbol{D}_{in} = \begin{bmatrix} w & d_{in} \\ w & d_{in} \\ \vdots & \vdots \\ w & d_{in} \end{bmatrix} \text{ and } \boldsymbol{C}_{in} = \begin{bmatrix} \gamma \\ \delta \end{bmatrix}. \tag{15}$$

IV. Results and Analysis

In this section the resulting path-loss models are determined from the measured data and the resulting curves are plotted. Shadowing parameters are also extracted from the data and model parameters are derived empirically. Tables II and III summarise the modelled path-loss parameters for each of the models and the corresponding RMSE values.

A. Model A

Table II summarises the resulting parameters for Model A obtained for the four frequencies of interest using data measured along both streets. It is noted that the average wall loss (γ) is higher for higher carrier frequencies, which is a generally accepted trend for common construction materials. Figure 2 shows a plot of the resulting Model A as well as the corresponding measured path-loss data for the case of the transmitter placed inside the room BR for each of the four carrier frequencies of interest and using the data obtained from both streets (RR and SC)). It is observed from the figure that there is good agreement between the measured and modelled path-loss, where the model results in a $bestfit$ curve representing the measured data.

TABLE II

Modelled parameters and RMSE for Model A

Modelled Parameters	Average Value			
	900 MHz	2 GHz	2.5 GHz	3.5 GHz
α (dB)	35.65	39.54	44.70	48.73
β	3.25	3.44	3.48	3.69
γ (dB/wall)	6.87	8.73	11.30	11.55
RMSE (dB)	6.93	9.06	8.93	8.45

B. Model B

Table III summarises the model parameters relating to Model B using data obtained from both streets for each of the four carrier frequencies. It is seen from Table III that the path-loss exponent (β), average wall loss (γ) and average internal propagation loss (δ) all increase with carrier frequency. Fig. 3 shows plots of the resulting Model B as well as the corresponding measured path-loss values when the transmitter was placed inside the room LR (2 walls) for each of the four carrier frequencies of interest, where figures are shown for each of the two streets. The curves in Fig. 3 show good correspondence between the measured and modelled path-loss values, where the curves are seen to approximate the mean value of the data points. It is also noted that the general trends are similar for each street, with variations occurring at larger distances. Note that this model

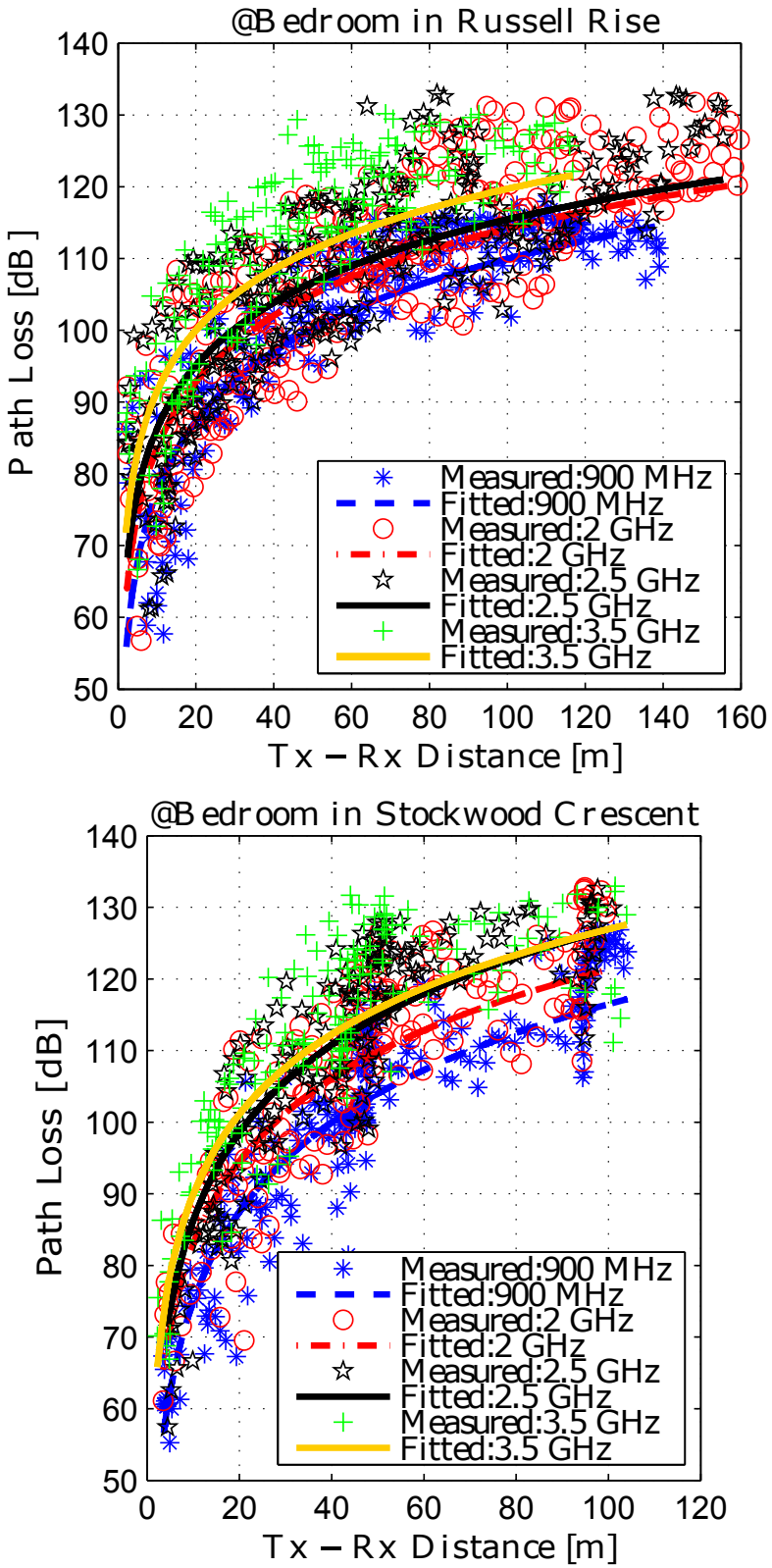

Fig. 2. Path-loss fitted by Model A of the measurement data when the transmitter was placed in the bedroom ($w = 1$, i.e. one wall)

explicitly incorporates a parameter for average internal propagation loss (δ), thus enabling the contribution of the average outdoor, indoor and wall losses to be determined and analysed independently.

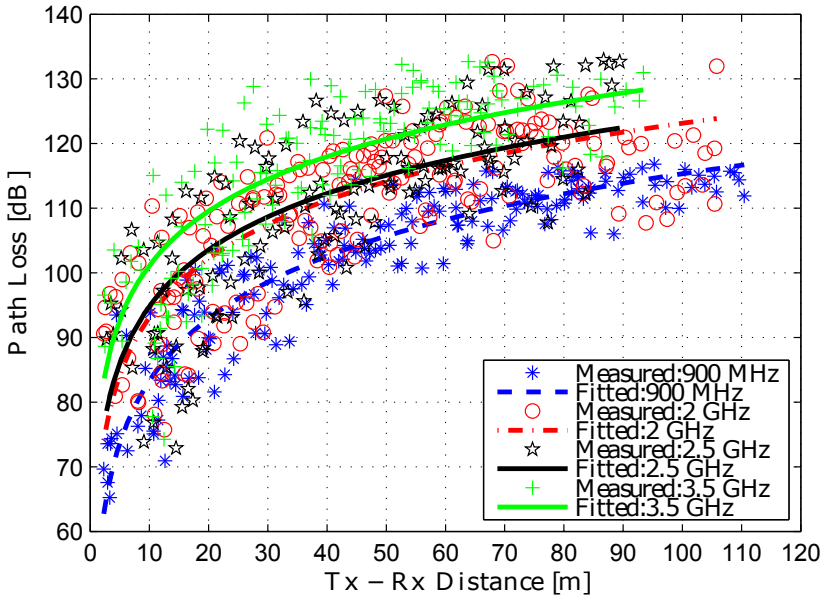

(a) Street 1 (Russell Rise)

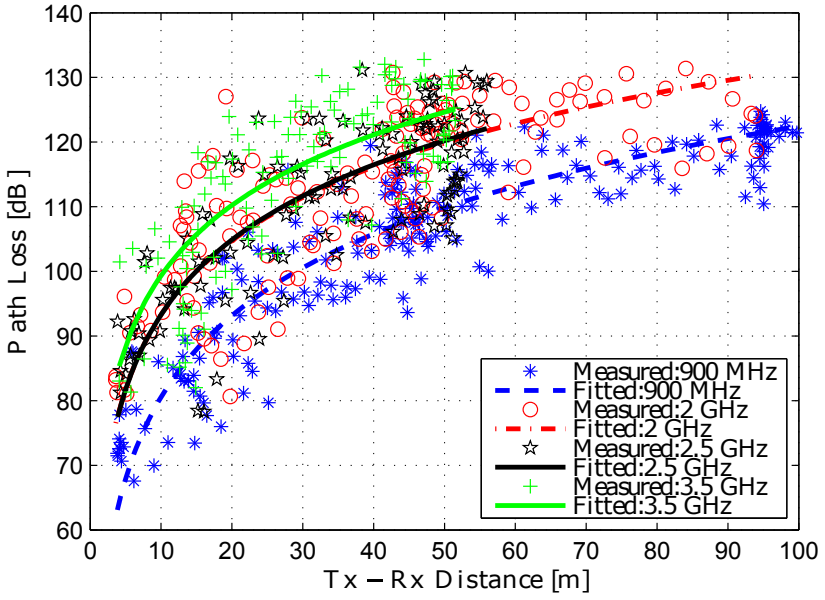

(b) Street 2 (Stockwood Crescent)

Fig. 3. Path-loss Model B and measured data when the transmitter was placed in the living room ($w = 2$, i.e. 2 walls) for each carrier frequency and for each road (RR and SC)

TABLE III

MODELLED PARAMETERS AND RMSE FOR MODEL B

Modelled Parameters	Average Value			
	900 MHz	2 GHz	2.5 GHz	3.5 GHz
α (dB)	34.93	38.86	43.78	46.64
β	3.21	3.40	3.44	4.68
γ (dB/wall)	5.01	5.29	5.85	11.21
δ (dB/m)	1.15	1.33	1.72	3.17
RMSE (dB)	6.75	8.87	8.84	7.94

C. Shadowing

Shadowing can be modelled as the random variation of the received signal power around the mean, where the variation usually fits a log-normal distribution [20]. Shadowing for the given scenarios can be analysed and modelled from the residuals of the path-loss data obtained from the measurements and the resulting fitted models, as indicated by expression (4). Figure 4 shows the resulting Cumulative Density Functions (CDF) of the residual path-loss data in dB's obtained from the measurement data, and the mean path-loss obtained using Model B for each of the two locations of interest (RR and SC), was well as that of an idealised normal distribution (which is a straight line) with parameters chosen to match as closely as possible to the data. The results show good correspondence for the majority of values, with deviations occurring at the extremities. The deviation is a consequence of the relatively low number of data points in these areas of the curve as well as the increased sensitivity to the operational environment at these extremities, i.e., SNR as low as 10 dB and increased likelihood of occlusion for the outdoor segment of the links. A closer fit may be obtained by using a distribution with more degrees-of-freedom. This would, however, make comparison with existing results more difficult and for this reason the Normal distribution has been retained. From Fig 4, it is noted that the residual path-loss data may be approximated by a Normal distribution with the mean of 0 dB and with a standard deviation equal to the RMSE value given in the corresponding tables. That is, Normal distribution $\mathcal{N}(\mu, \sigma^2)$, with μ representing the mean and σ the standard deviation. By way of example, Table IV shows the shadow fading distribution relating to the residual values of Model B at 99 % confidence interval and 0 dB mean for each of the street (RR and SC). Thus, the signal level variance around the 0 dB mean is (-18.8, 21.7) dB of 99 % of occurrences for the 900 MHz Russel Rise data, as can be established from Fig 4a. Such a model is helpful in the estimation of extreme interference levels, and models may be derived with other confidence levels chosen to be appropriate for the operational conditions of interest.

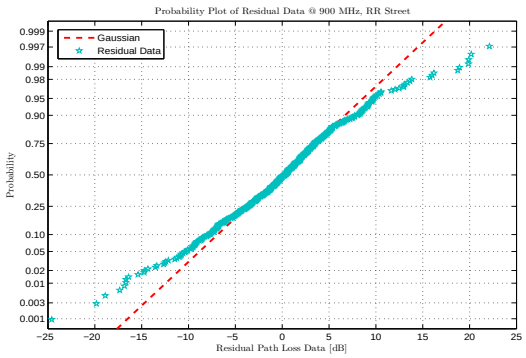

(a) At 900 MHz in Russel Rise

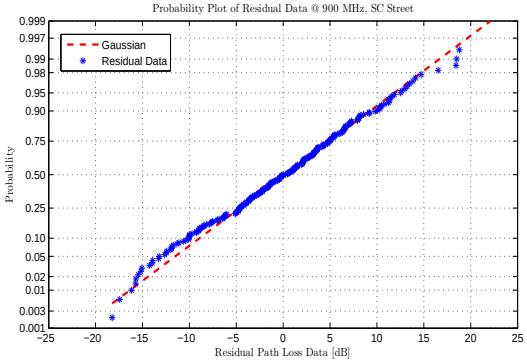

(b) At 900 MHz in Stockwood Crescent

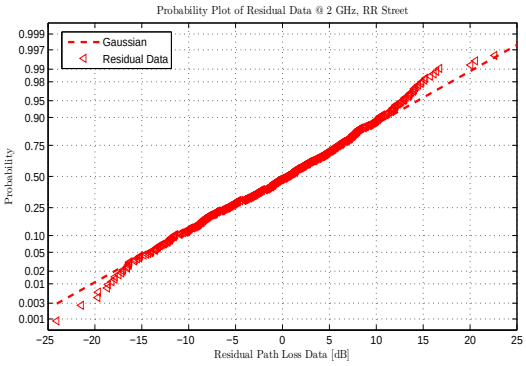

(c) At 2 GHz in Russel Rise

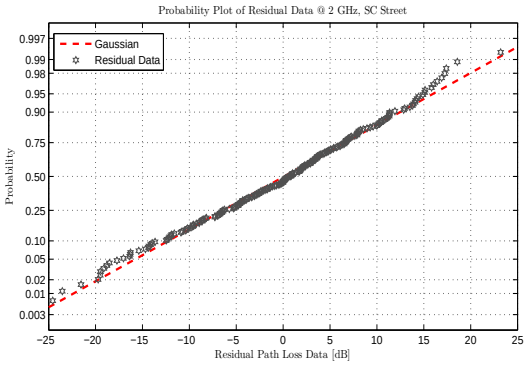

(d) At 2 GHz in Stockwood Crescent

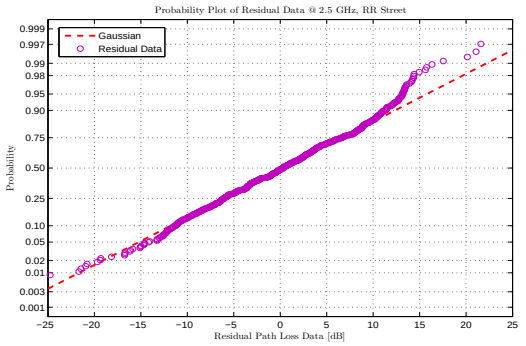

(e) At 2.5GHz in Russel Rise

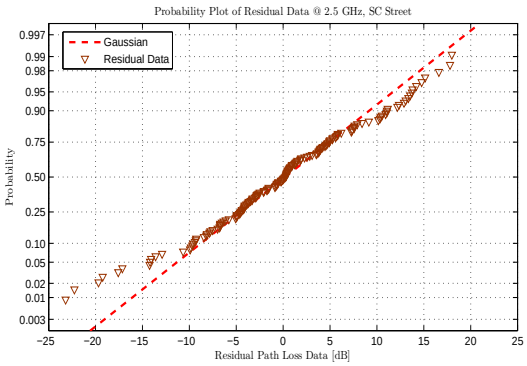

(f) At 2.5 GHz in Stockwood Crescent

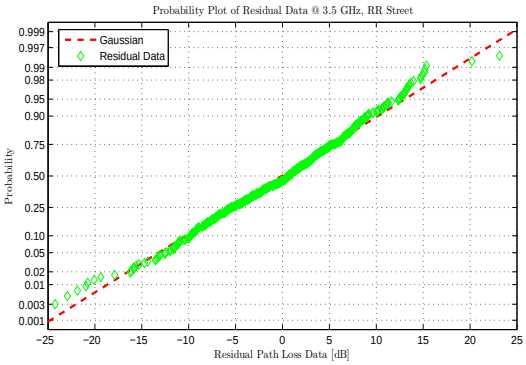

(g) At 3.5 GHz in Russel Rise

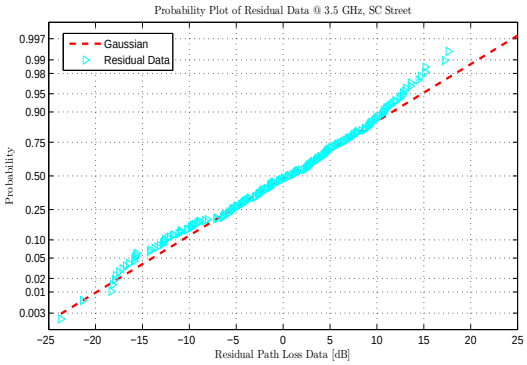

(h) At 3.5 GHz in Stockwood Crescent

Fig. 4. CDF of the residual path-loss data from model B for the carrier frequencies of interest and for each location (RR and SC). Idealised Gaussian model is also depicted.

D. Model Validation

The accuracy of the two path-loss models may be evaluated by considering the RMSE. For comparison, the RMSE values, which corresponds to the standard deviation of the shadowing, are compared with those obtained in Valcarce's model [13]. This is chosen as the benchmark because the same set of measurement data has been used to form Valcarce's model and so a direct comparison in terms of RMSE between the two approaches is possible. Table V shows that the RMSE obtained from the models derived in this paper are comparable with the RMSE values obtained by Valcarce's model, where it can be seen that the RMSE values obtained by using the SVD approach are 0.3 - 2.1 dB's less than those obtained in [13]. This is because [13] uses 7 degrees of freedom to model the path-loss over a 118 % fractional frequency bandwidth (see definition in [21]). Whereas we have considered each band independently and with physically attributable parameters. Table V presents parameters obtained for the four carrier frequencies of interest and has also partitioned the data and resulting models between the two locations (RR and SC). Furthermore, the WINNER II path-loss model described in [8] claims a standard deviation of 7 dB for the frequency range of 2-6 GHz, however the work in [8] differs in terms of antenna height and operational environment and so can be considered as a guideline rather than a conclusive observation. The parameters that result from the modelling work presented in this paper provide insights into wall loss and internal building propagation loss. For example, both of these parameters are seen to increase with frequency, however the resulting parameters should be treated as average values and should not be used to give definitive wall loss values for any specific wall. This is because the angle of propagation through the walls and the type of building material (e.g. inner and outer wall materials) vary throughout the measurements and there is also the possibility of multiple reflected signals passing through the walls at differing locations and angles. The walls may also have a non-uniform construction, i.e., the provision of a door or window. It is clear that inaccuracies would be present in models because the assumption has been made that the number of walls the signal passes through is 1 or 2. This may be considered to be valid for when the receiver is located directly outside the building, but when it is located along the street additional loss would be incurred due to occlusion from surrounding buildings etc. Thus, for these cases wall loss may be better attributed as a bulk loss that includes the main building wall losses as well as losses incurred by objects causing additional occlusion to the link.

The resulting path-loss models have additionally been compared with measured path-loss data and subsequent model obtained at 2.5 GHz and obtained from an entirely independent measurement campaign. These measurements took place at the University of Durham, UK using independent equipment, different setting and building geometry, but similar materials. The femtocell operating scenario was retained. The channel sounder in [17] was used with a 500 MHz channel bandwidth and 1.2 kHz repetition rate to log a total of 30 data points covering line-of-sight, as well as one and two brick walls. The measurements

are limited to a maximum of 33 m, due to the physical restrictions imposed by near-by buildings. Path-loss was estimated by taking the area under the power delay profile. The best-fit curve was then determined based on a power law model to be (in dB)

$$L_p = 62.28 + 3.2310 \cdot 10\log_{10}(d), \tag{16}$$

This gives an RMSE of 3.05 dB. Figure 5 shows plots of the resulting path-loss curves at 2.5 GHz for both sets of measurement data, and for the case of one wall between the transmitter and receiver. The difference between the curve representing the Durham measurement data and the other two curves may be attributed to the difference in building construction, i.e., wall thickness and building geometry. Incidence angle and clutter also contribute to resulting path-loss curves. Note that the curves relating to the models developed in this paper are almost identical. Although numerical differences are evident when examining the data to at least one decimal place, the similarity of the curves is considered to contribute to validating the models.

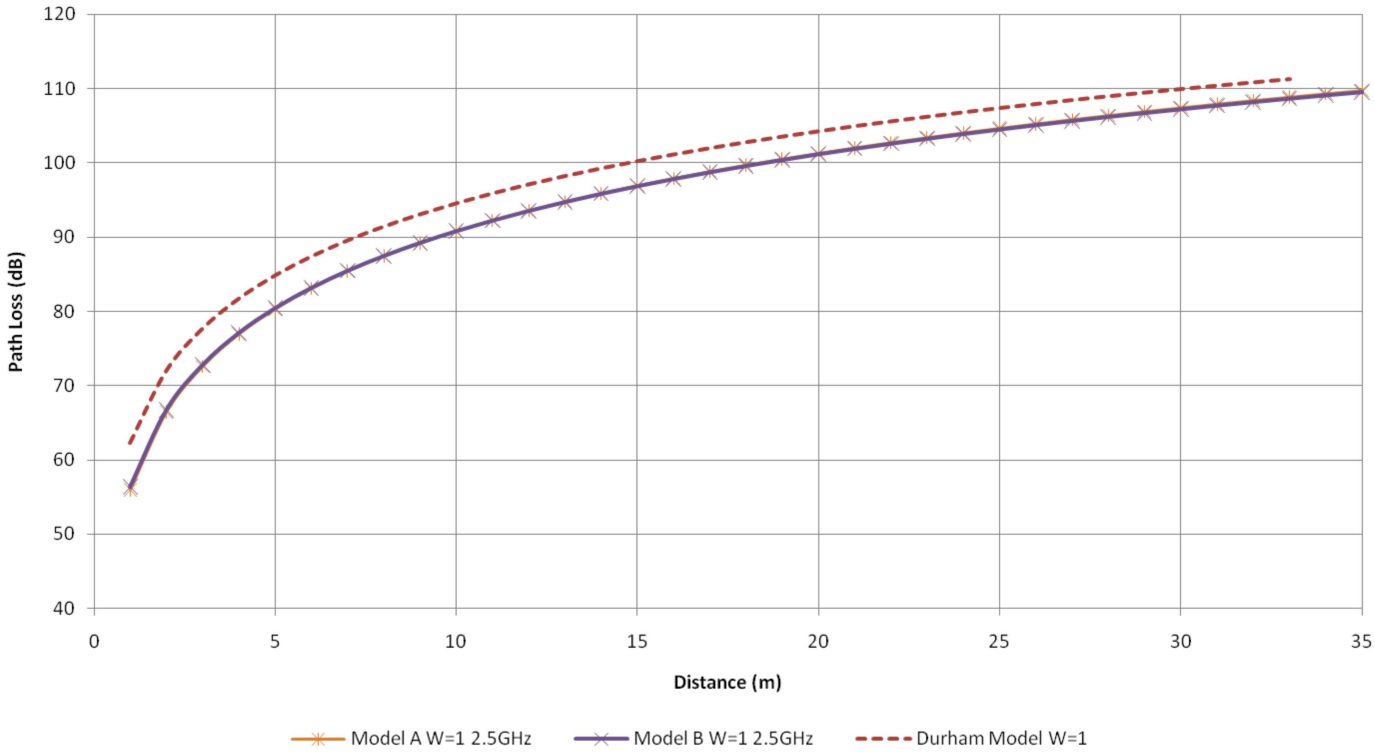

Fig. 5. Comparison of Path Loss Models at 2.5GHz and with a single wall used in all the models, i.e. W=1

TABLE IV

THE 99 % CONFIDENCE INTERVAL OF THE SHADOW FADING DISTRIBUTION

Shadow Fading Boundary in dB at 99 % Confidence Interval				
Street	900 MHz	2 GHz	2.5 GHz	3.5 GHz
RR	(-18.8, 21.7)	(-25.7, 29.4)	(-27.2, 31.5)	(-22.8, 26.6)
SC	(-20.3, 23.3)	(-25.7, 30.0)	(-23.5, 28.7)	(-23.0, 27.6)

TABLE V

COMPARISON OF AVERAGE RMSE VALUE WITH VALCARCE'S PATH-LOSS MODEL IN [13]

Model	900 MHz	2 GHz	2.5 GHz	3.5 GHz
Valcarce's model (dB)	8.7	10.5	10	10
Model A (dB)	7.5	9.1	9.4	8.5
Model B (dB)	7	8.8	9.7	7.9

V. CONCLUSIONS

This paper has presented two empirical path-loss models for a femtocell indoor-to-outdoor scenario in an urban environment and for carrier frequencies of 900 MHz, 2 GHz, 2.5 GHz and 3.5 GHz. The models have been developed from a set of continuous wave received power measurement data. The Singular Value Decomposition (SVD) method was adopted in the modelling of the measurement data, which has not been considered in any of the existing literature relating to path-loss modelling. The two models defined by equations (7), (9) with parameters given in Tables II, and III may be used to study the interference level from a 3G/4G femtocell to a macrocell user in a residential urban environment.

From the PDF and the CDF of the residual path-loss data, it was found that the behaviour of the shadowing approximates a Log-normal distribution with 0 dB mean and RMSE value in dB as the standard deviation, which varies depending on the operational scenario and carrier frequency. The boundary value of the shadowing distribution at a 99 % confidence interval provides an insight into the estimation of extreme interference levels. For example, the extreme variation of signal level around the mean at 900 MHz frequency in Russell Rise street is (-18.8, 21.7) dB for 99 % of occurrences.

The results demonstrate good agreement with related models, and have integrated SVD into the process of path-loss modelling for the first time, and which has been shown as a convenient means of deriving shadowing characteristics as well as path-loss model parameters. They may be used in conjunction with other existing models such as the WINNER II model to cover a wide range of operating frequencies in the range of 900 MHz to 6 GHz with good accuracy and for a range of operational scenarios relating to femtocell deployments.

ACKNOWLEDGMENT

The authors would like to acknowledge Dr. Alvaro Valcarce for driving the measurement campaign conducted by the University of Bedfordshire in Luton, United Kingdom, which has provided the data used for the work presented here. We would also like to acknowledge the support and guidance provided by Dr Enjie Liu throughout the initial development of the models and with the initial formation of this paper.

REFERENCES

[1] J. Zhang and G. de la Roche, *Femtocell: Technologies and Deployment*, 1st ed. John Willey & Sons, Dec. 2009, ISBN 978-0470742983.

[2] G. H. Golub and W. Kahan, "Calculating the singular values and pseudo-inverse of a matrix," *Journal of the Society for Industrial and Applied Mathematics: Series B*, vol. 2, pp. 205–224, Feb. 1965.

[3] K. Baker, "Singular Value Decomposition Tutorial," Ohio State University, Jan. 2013, http://www.ling.ohio-state.edu/~kbaker/pubs/Singular_Value_Decomposition_Tutoria

[4] D. P. McNamara, M. A. Beach, P. N. Fletcher, and P. Karlsson, "Capacity variation of indoor multiple-input multiple-output channels," *IET Electronics Letters*, vol. 2, pp. 2037 – 2038, Nov. 2000.

[5] G. de la Roche, A. A.-Glazunov, and B. Allen, *LTE-Advanced and Next Generation Wireless Networks: Channel Modelling and Propagation*, 1st ed. John Willey & Sons, Nov. 2012, ISBN 9781119976707.

[6] G. D. Durgin, T. S. Rappaport, and H. Xu, "Partition-Based Path Loss Analysis for In-Home and Residential Areas at 5.85 GHz," in *Global Telecommunications Conference (GLOBECOM, IEEE)*, vol. 2, 1998, pp. 904–909.

[7] D. M. Rose, T. Jansen, and T. Kurner, "Indoor to Outdoor Propagation - Measuring and Modeling of Femto Cells in LTE Networks at 800 and 2600 MHz," in *GLOBECOM Workshops (GC Wkshps, IEEE)*, Dec. 2011, pp. 203–207.

[8] P. Kyösti *et al.*, "WINNER II Channel Models Part II Radio Channel Measurement and Analysis Results," WINNER II Public Deliverables, Sep. 2007.

[9] L. A. Linares and J. G. Sanchez, "Empirical Modeling of Femtocell Path Loss in a Femto-to-Macro Indoor-to-Outdoor Interference Scenario," Master Thesis, University of Aalborg, Aalborg, Denmark, May 2011.

[10] Ofcom, "Predicting Coverage and Interference Involving the Indoor-Outdoor Interface," OFCOM, Ofcom Project SES-2005-08 Final Report v.1.0, Jan. 2007.

[11] ITU-R P.1238, "Propagation Data and Prediction Methods for the Planning of Indoor Radiocommunication Systems and Radio Local Area Networks in the Frequency Range 900 MHz to 100 GHz," ITU, Recommendation ITU-R P Series Radiowave Propagation, Feb. 2012.

[12] Y. Corre, J. Stephan, and Y. Lostanlen, "Indoor-to-Outdoor Path-Loss Models for Femtocell Predictions," in *Personal Indoor and Mobile Radio Communications (PIMRC, IEEE 22nd)*, Sep. 2011, pp. 824–828.

[13] A. Valcarce and J. Zhang, "Empirical Indoor-to-Outdoor Propagation Model for Residential Areas at 900.-3.5 GHz," *IEEE Antennas and Wireless Propagation Letters*, vol. 9, pp. 682–685, 2010.

[14] G. de la Roche, P. Filipo, Z. Lai, G. Villamaud, J. Zhang, and J. Gorce, "Implementation and validation of a new combined model for outdoor to indoor radio coverage predictions," *EURASIP Journal on Wireless Communications and Networking*, 2010.

[15] ITU-R P.2040, "Effects of building materials and structures on radiowave propagation above about 100 MHz," ITU-R, Recommendation, Jul. 2015.

[16] Ericsson, "World's First Commercial LTE-Advanced Call on 1800 MHz and 900 MHz," Press Release, 12 Aug. 2013, http://hugin.info/1061/R/1722258/573811.pdf.

[17] S. Salous, A. Cheema, and X. Raimundo, "Radio channel propagation measurements using a multiband agile chirp sounder," in *General Assembly and Scientific Symposium (URSI GASS), 2014 XXXIth URSI*, Aug. 2014, pp. 1 – 4.

[18] A. Valcarce, "Applying the Finite-Difference Time-Domain to the Modelling of Large-Scale Radio Channels," PhD Thesis, University of Bedfordshire, Luton, UK, Aug. 2010.

[19] Cobham, "Cobham Antenna Systems," Feb. 2010, http://www.european-antennas.co.uk/.

[20] J. Salo, L. Vuokko, H. M. El-Sallabi, and P. Vainikainen, "An Additive Model as a Physical Basis for Shadow Fading," *IEEE Trans. Veh. Technol.*, vol. 56, no. 1, pp. 13–26, Jan 2007.

[21] B. Allen, M. Dohler, E. Okon, W. Malik, A. Brown, and D. Edwards, *Ultra-wideband Antennas and Propagation for Communications, Radar and Imaging*, 1st ed. United Kingdom: Wiley, Oct. 2007.